Group B Streptococcal β-Hemolysin Induces Mortality and Liver Injury in Experimental Sepsis

Axel Ring,[1,4] Johann S. Braun,[5] Jürgen Pohl,[4] Victor Nizet,[3] Wolfgang Stremmel,[4] and Jerry L. Shenep[1,2]

[1]Department of Infectious Diseases, St. Jude Children's Research Hospital, and [2]Department of Pediatrics, University of Tennessee, Memphis; [3]Division of Pediatric Infectious Diseases, University of California, San Diego; [4]Department of Internal Medicine IV, Ruprecht-Karls-University, Heidelberg, and [5]Department of Neurology, Humboldt University, Berlin, Germany

New Zealand White rabbits were challenged with the wild-type (wt) group B streptococci (GBS) serotype III strain (COH1) and its isogenic nonhemolytic (NH) and hyperhemolytic (HH) mutants. Mortality differed significantly between rabbits infected with the HH mutant IN40 (67%), compared with rabbits infected with the wt COH1 strain (27%) and the NH strains COH1-20 and COH1:*cyl*EΔ*cat* (13% and 0%, respectively; $P < .05$). Histopathologically, disseminated septic microabscesses surrounded by necrotic foci were found exclusively in the livers of HH mutant IN40–infected animals. Serum transaminase levels were 20-fold higher in the HH-infected group, compared with rabbits infected with the other strains. Positive TUNEL (in situ terminal deoxynucleotide transferase–mediated dUTP nick end labeling) staining and activation of caspase-3 in hepatocytes were more frequent in HH-infected than in wt-infected animals and absent in the NH mutant COH1-20–infected group, indicating that GBS β-hemolysin triggers apoptotic pathways in hepatocytes. This work provides the first evidence that GBS β-hemolysin plays a crucial role in the pathophysiology of GBS sepsis by inducing liver failure and high mortality.

On an annual basis, sepsis syndrome is diagnosed in ~1,000,000 patients in Europe and the United States. The incidence of gram-positive sepsis has risen since the 1980s, and, today, gram-positive organisms cause ~50% of all cases of sepsis [1]. Group B streptococci (GBS; *Streptococcus agalactiae*) are a major etiologic agent of pneumonia, meningitis, and septic shock in human newborn infants. The most thoroughly studied virulence factor of GBS is its antiphagocytic capsule [2], but the purified capsular polysaccharide is relatively innocuous, with regard to host injury. Like other gram-positive bacteria, GBS possess the cell-wall components peptidoglycan and lipoteichoic acid, with potentially toxic properties [3]. High concentrations of peptidoglycan and lipoteichoic acid of *Staphylococcus aureus* and *Streptococcus pneumoniae,* which seldom occur clinically, have been shown to induce characteristic signs of septic shock, such as hypotension, multiple organ dysfunction, and induction of inducible nitric oxide (NO) synthase (iNOS), in a rat model [4]. The cell walls of species that rarely cause septic shock, despite the fact that they commonly invade the bloodstream (e.g., *Staphylococcus epidermidis*), have not been demonstrated to be less toxic than the structurally similar components of highly virulent organisms. Thus, although cell walls may contribute to gram-positive septic shock, their effects do not fully explain the propensity of highly virulent pathogens, including GBS, to cause septic shock. Only recently has the effect of exotoxins been recognized in the context of classic streptococcal septic shock [5]. For instance, toxic shock syndrome is clinically indistinguishable from bacteremic shock, and this process is thought to be mediated solely by trace quantities of absorbed exotoxins that are produced by certain strains of *S. aureus* or group A streptococci [6].

Virtually all clinical isolates of GBS express a β-hemolytic phenotype on blood plates [7]. GBS β-hemolytic activity is mediated by a novel pore-forming cytotoxin, the genetic basis of which has been elucidated elsewhere [8–10]. In vitro, GBS β-hemolysin activity is associated with injury to lung epithelial [11] and endothelial [12] cells and to brain endothelial cells [13] and thus is speculated to contribute to GBS penetration of host cellular barriers [14]. We found recently that GBS β-hemolysin expression is associated with the induction of NO release from murine macrophages [15] and interleukin-8 from human lung epithelial cells [16], suggesting that β-hemolysin may also exhibit proinflammatory properties relevant in the sepsis cascade.

In an adult mouse model of late-onset GBS bacteremia and arthritis, β-hemolysin expression was associated with increased mortality, increased joint damage, and increased blood and intra-articular levels of interleukin-6 [17]. Information on the requirement(s) of GBS β-hemolysin expression for the more common and clinically important syndrome of early-onset septicemia,

Received 28 June 2001; revised 31 January 2002; electronically published 22 May 2002.

Experiments were performed according to a protocol approved by the Animal Care and Use Committee at St. Jude Children's Research Hospital.

Financial support: National Institutes of Health (AI-27913 to J.L.S. and AI-01451 to V.N.); Cancer Support CORE grant (CA-21765 to St. Jude Children's Research Hospital); American Lebanese Syrian Associated Charities.

Reprints or correspondence: Dr. Axel Ring, Ruprecht-Karls-University, Dept. of Internal Medicine IV, Bergheimer Strasse 58, Heidelberg, Germany 69115 (axel_ring@med.uni-heidelberg.de).

The Journal of Infectious Diseases 2002;185:1745–53

0022-1899/2002/18512-0008$02.00

however, is scant. Partially purified, β-hemolysin–containing supernatants of GBS cultures have been shown to induce cardiotoxicity and hypotension after intravenous administration into rabbits and rats [18]. Small-scale experiments using live GBS in neonatal rats gave conflicting results: nonhemolytic (NH) mutants were less virulent than the parent strain after direct pulmonary (transthoracic) injection [19] but no less virulent after intravenous administration [7]. In the present study, we used isogenic GBS mutants to examine the role of β-hemolysin in the course of experimental GBS septic shock.

Material and Methods

Bacterial strains. COH1, a highly encapsulated type III GBS strain isolated from the blood of a neonate with sepsis, was used in this study [20]. Hyperhemolytic (HH; IN40) and NH (COH1-20) isogenic variants of this isolate were produced by a single random insertion of Tn916ΔE into the chromosome of the parent isolate [11]. These mutations have been mapped (V.N., unpublished data) and are distinct from the *cyl* locus containing the newly discovered GBS β-hemolysin structural gene *cyl*E. Although the molecular genetic link to altered β-hemolysin activity remains uncertain, the mutants are identical to the parent strain in terms of logarithmic growth rate, production of capsule, group B antigen and hyaluronidase, and the enzymatic and sugar fermentation profiles on the Api 20 Strep system for identification of streptococci (BioMérieux) [11, 12]. The genetically defined *cyl*E knockout mutant COH1:*cyl*EΔ*cat* was generated by targeted plasmid integrational mutagenesis, as described by Pritzlaff et al. [10]. On the spectrum of GBS clinical isolates, the COH1 strain produces a relatively modest baseline level of β-hemolysin activity. The HH mutant IN40 expressed ~100-fold greater levels of β-hemolysin, levels comparable to those in other robustly hemolytic wild-type (wt) strains that have been characterized elsewhere [11]. The strains were grown to late logarithmic phase (optical density at 620 nm, 0.8, corresponding to 2×10^8 cfu/mL), as assessed by the limulus amebocyte lysate test, in the semisynthetic casein and yeast medium [21], which did not contain any detectable contaminating endotoxin (< 0.05 EU/mL).

Experimental infection of rabbits. New Zealand White rabbits weighing ~3 kg were anesthetized by intramuscular injection of ketamine (50 mg/kg), xylazine (10 mg/kg), and acepromazine (1.5 mg/kg). Anesthesia was maintained with these substances (25 mg/kg ketamine, 5 mg/kg xylazine, and 0.75 mg/kg acepromazine per single dose, as needed). Rabbits spontaneously breathed room air throughout the experiment. Indwelling catheters were surgically placed into the femoral artery and vein immediately before induction of sepsis. A double-lumen 4-French polyurethane catheter in the femoral vein was used to inject the bacteria; the arterial catheter was used for blood sampling and continuous monitoring of systolic, diastolic, and mean arterial blood pressure.

Bacterial strains grown in casein and yeast medium were washed twice in PBS before injection into rabbits. Sepsis was induced by intravenous infusion of an aliquot of a freshly prepared GBS suspension (10^9 cfu in 10 mL PBS per rabbit), which was held on ice until use. Control animals received PBS only. Forty-five rabbits were studied in replicates of 3 animals, with each member of a set being challenged with wt strain COH1, HH mutant IN40, or NH mutant COH1-20 by blinded, random assignment. Two additional groups of rabbits were studied: 12 rabbits were studied after challenge with COH1:*cyl*EΔ*cat* when this defined mutant subsequently became available, and 6 rabbits received sham challenge. Rabbits surviving for 8 h after bacterial challenge were killed while under anesthesia by intravenous injection of pentobarbital (75 mg/kg). Investigators remained blinded until each experimental set was completed. Immediately before and 30, 90, 180, and 480 min after bacterial challenge, 1.5-mL samples of blood were obtained from each rabbit for quantitative culture and determination of nitrite/nitrate and lactic acid concentrations. Additional 200-μL samples of blood were obtained at 0, 30, and 480 min for complete blood cell counts, and 3-mL specimens for determination of clinical chemistry parameters were obtained prior to challenge and at the end of the experiments (480 min).

Hematoxylin-eosin (H-E), activated caspase-3, and TUNEL stains. Liver tissue specimens were fixed in 10% neutral-buffered formalin, embedded in paraffin, sectioned at 5 μm, stained with H-E, and examined by light microscopy. Activated caspase-3 in liver sections was detected by using an affinity-purified antibody against active caspase-3 (1 μg/mL; PharMingen). The Vectastain Elite ABC kit (Vector) was used to visualize primary antibody binding sites. The ApopTag in situ apoptosis detection kit (Intergen) was used to detect apoptotic nuclei with fragmented DNA, according to the manufacturer's instructions. The terminal transferase adds digoxigenin-labeled and unlabeled nucleotides to the DNA fragments' free 3′-OH ends. Binding of digoxigenin nucleotides was visualized with a peroxidase-conjugated anti-digoxigenin antibody and diaminobenzidine.

Measurement of bacteremia. Serial 10-fold dilutions of each blood sample were prepared with PBS containing 1% albumin; 0.1 mL of each dilution was cultured on a chocolate agar plate, and colony-forming units were counted after overnight incubation at 37°C.

Lactic acid and nitrite/nitrate assays. The 1.5-mL blood specimens were centrifuged in a tabletop centrifuge to remove all cellular constituents. The supernatants were passed through a Centricon filter (cutoff, 10,000 daltons; Amicon) for deproteinization. The lactate concentration was determined in the clear filtrate, using a blood lactic acid kit (826-UV; Sigma). For determination of nitrite concentrations with the Griess reaction, nitrate was reduced to nitrite according to the following protocol: 10 μL of nitrate reductase (5 U/mL; Sigma) and 10 μL of NADPH (12 mmol/L; Sigma) were incubated with 100 μL of the deproteinized sample for 30 min at 37°C. Next, 10 μL of lactic dehydrogenase (350 U/mL; Sigma) and 10 μL of pyruvate (700 mmol/L; Sigma), together with 60 μL of PBS, were added to the solution and incubated for another 15 min at 37°C. Nitrite was quantified with the Griess reaction, as described elsewhere [22].

Complete blood cell counts and clinical chemistry. The blood specimens for complete blood cell counts were placed in glass tubes containing heparin and analyzed by use of an automatic counter (Sysmex CC-180-A; TOA Medical Electronics). Serum clinical chemistry parameters were determined by MedLabs (Memphis).

Statistical analysis. Data presented are means ± SD of 5–15 measurements (depending on the number of surviving rabbits at a given time point). Analysis of variance was used to determine the significance of differences between clinical parameters. The Kaplan-

Meier survival plot was analyzed by the log rank test. $P < .05$ was considered to be significant.

Results

HH GBS challenge of rabbits is associated with increased mortality. After intravenous infusion of 10^9 cfu of the HH mutant IN40, death occurred in 10 (67%) of 15 rabbits within the observation period of 8 h. In contrast, rabbits injected with the wt strain COH1 showed a mortality rate of only 27% (4/15), whereas the NH mutants COH1:*cyl* EΔ*cat* and COH1-20 induced the lowest mortality rate, 0 (0%) of 12 and 2 (13%) of 15, respectively (figure 1). Mortality was also zero in the sham-treated group.

Thirty minutes after injection of GBS, bacteremia was at a level of ~10^5 cfu/mL blood in the COH1, IN40, and COH1-20 groups but only 2.5×10^4 cfu/mL in the COH1:*cyl* EΔ*cat* group (figure 2). In the COH1-20 group, bacteremia declined to 2.5×10^3 cfu/mL after 3 h, indicating that this mutant was unable to establish progressive, high-grade bacteremia. In contrast, the concentration of the *cyl* E knockout mutant COH1:*cyl* EΔ*cat* rose to ~4×10^5 cfu/mL after 8 h, following a nadir at 90 min postinfection (figure 2). The wt strain COH1 resulted in the highest bacteremia, amounting to 6×10^5 cfu/mL after 8 h. In the group infected with HH strain IN40, only 33% of animals survived the 8-h period, with a mean bacteremia of 10^4 cfu/mL, indicating that strain IN40, compared with the COH1 and COH1:*cyl* EΔ*cat* strains, induces substantially higher mortality without an apparent advantage in establishing and maintaining bacteremia.

Hypotension occurs independently of GBS β-hemolysin production. Since GBS β-hemolysin is a potent inducer of iNOS expression and NO production in murine macrophages [15], we hypothesized that β-hemolysin might play a role in the pathogenesis of septic shock by stimulating in vivo NO release with consequent severe hypotension. However, the mean arterial pressure declined steadily over 8 h to ~50% of the original level (figure 3) in the wt strain COH1, HH mutant IN40, and NH mutant COH1-20 groups independently of β-hemolysin expression. Likewise, the serum nitrite concentrations in septic rabbits increased ~3-fold during the 8-h experiment, with no significant differences among the 3 treatment groups (table 1). Treatment with the COH1:*cyl* EΔ*cat* mutant resulted in a lesser decrease of mean arterial pressure, compared with the other GBS strains investigated (figure 3).

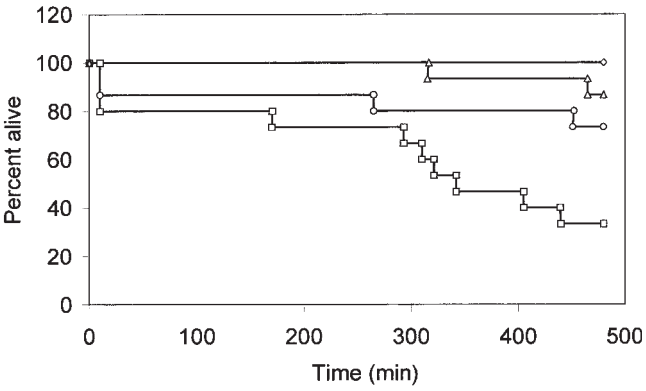

Figure 1. Kaplan-Meier plot of survival in the rabbit group B streptococcal septic shock model. Rabbits were injected with the IN40 (□), COH1 (○), COH1-20 (△), or COH1:*cyl* EΔ*cat* (◇) strain of group B streptococci. The total no. of animals was 15 each for the COH1, IN40, and COH1-20 groups and 12 for the COH1:*cyl* EΔ*cat* group. The differences between IN40 and COH1, COH1-20, or COH1:*cyl* EΔ*cat* were statistically significant ($P < .05$, log-rank test).

Clinical laboratory monitoring. Leukocyte and platelet counts declined to a similar degree during the course of the experiment in all 3 groups (table 1). Hemoglobin levels and red blood cell counts remained constant in the 3 groups (table 1). Thus, GBS do not cause clinically apparent hemolysis in vivo, even when producing relatively large amounts of β-hemolysin. However, lactic dehydrogenase increased 66-fold in the HH mutant IN40 group and < 10-fold in the wt strain COH1 and NH mutant COH1-20 groups (table 1), suggesting that cell death occurs in a β-hemolysin–dependent fashion. The accumulation of plasma lactate in animals of the wt strain COH1, HH mutant IN40, and NH mutant COH1-20 groups indicates impaired tissue perfusion independently of the level of β-hemolysin production (table 1). Creatinine increased moderately (but statistically significantly) above the normal range in the HH group, suggesting that moderate renal dysfunction might be associated with high-level β-hemolysin expression. The serum activities of aspartate aminotransferase and alanine aminotransferase increased 260- and 26-fold, respectively, in the HH mutant IN40 group but only mildly in the NH mutants COH1-20 and COH1:*cyl* EΔ*cat* and wt strain COH1 groups (table 1), indicating that extensive hepatocellular damage was correlated with β-hemolysin production. The serum levels of bilirubin, amylase, and lipase increased ~1.5-fold, compared with baseline levels, in all treatment groups but never exceeded the normal range (data not shown). Serum electrolytes were not affected by treatment with GBS (data not shown).

Histopathology of the liver. The serum chemistry parameters indicated that β-hemolysin–induced injury preferentially targets the liver parenchyma, without marked effects on biliary excretion or pancreatic function. Consequently, we characterized liver injury by H-E, TUNEL, and activated caspase-3 stains.

H-E stains. By light microscopy, disseminated septic microabscesses containing large amounts of bacteria surrounded by necrotic areas were found in peripheral segments of the livers from rabbits infected with the HH mutant IN40 (figure 4). On the level of the hepatic lobule, the necrotic areas were preferentially located around the portal triad (figure 4). In contrast, only a few isolated microabscesses were present in the liver of rabbits receiving the wt strain COH1 producing low amounts of β-hemolysin, and no areas of necrosis were evident (figure 4). Infiltration of mononuclear cells and polymorphonuclear neutrophil granulocytes in sinusoids and cytoplasmic vacuolization of hepatocytes

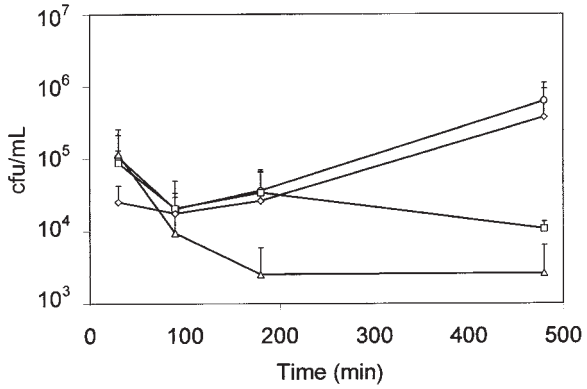

Figure 2. Bacteremia in rabbits treated intravenously with 10^9 cfu of the COH1 (○), COH1-20 (△), COH1:*cyl* EΔ*cat* (◇), or IN40 (□) strain of group B streptococci. Bacterial counts were determined by quantitative cultures on chocolate agar plates. Data are mean ± SD of all surviving rabbits per group ($n = 5–15$).

was detected both in the HH mutant IN40 and wt strain COH1 treatment groups. Liver histopathology in rabbits treated with the NH mutants COH1-20 and COH1:*cyl* EΔ*cat* was largely inconspicuous. In these groups, minimal neutrophil infiltrates and vacuolization were present in a minor number of rabbits, whereas the majority showed no abnormality (figure 4). Microabscesses or areas of necrosis were never found after treatment with the NH strains.

TUNEL staining. Livers of sham-treated rabbits and animals infected with NH mutant COH1-20 were negative, as determined by TUNEL staining (figure 5). In contrast, positive TUNEL staining was found in hepatocytes of animals infected with the HH mutant IN40 (figure 5). In contrast to the massive necrotic areas identified by the H-E stain, TUNEL-positive hepatocytes were scattered over the liver acini and not clustered in the periportal regions (figure 5). Morphologically, the TUNEL-positive hepatocytes were shrunken and had pyknotic nuclei (figure 5). Compared with the group infected with the HH mutant IN40, the livers of animals infected with the wt strain COH1 showed fewer TUNEL-positive hepatocytes, and the TUNEL-positive cells were frequently localized in clusters around the portal triad of the liver lobules (figure 5).

Immunohistochemical detection of activated caspase-3. Active caspase-3 staining was most abundant in hepatocytes of HH mutant IN40–infected livers (figure 6), with a predominantly pan-cytoplasmic pattern on a single cell level. In the group infected with HH mutant IN40, caspase-3–positive hepatocytes were distributed randomly within the liver parenchyma, with no anatomical relationship to a particular zone of the hepatic lobule (figure 6).

Positive staining of activated caspase-3 in hepatocytes of wt strain COH1–treated animals was less abundant, compared with that for the group infected with HH mutant IN40 (figure 6), showing mainly a punctate pattern of distribution on the single cell level. In contrast to the group infected with HH mutant IN40, the caspase-3–positive cells in the group infected with wt strain COH1 were concentrated around the portal triad (figure 6). In control livers and in livers infected with NH mutant COH1-20, no significant staining of activated caspase-3 was detected (figure 6).

Discussion

On the basis of our previous in vitro studies showing that the β-hemolysins of both GBS and *S. pneumoniae* are potent inducers of iNOS and NO production in macrophages [15, 23], we hypothesized that GBS β-hemolysin might play a role in the pathophysiology of sepsis and septic shock. To investigate this hypothesis, we used the GBS wt strain COH1 and its isogenic NH (COH1-20 and COH1:*cyl* EΔ*cat*) and HH (IN40) mutant strains in a lapin model of sepsis.

The COH1-20 and IN40 mutants were generated by a single random insertion of Tn916ΔE into the chromosome of the parent isolate [11]. These mutations have been mapped (V.N., unpublished data) and are distinct from the *cyl* locus containing the newly discovered GBS structural gene *cyl* E. The NH mutant COH1-20 maps to an intragenic fragment 100 bp upstream of a large open-reading frame with homologies to the *Streptococcus thermophilus* lactose transport system protein (40% identity and 75% similarity). The identical insertion was identified in the NH mutants COH31cl5 and COH31cl12 reported by Weiser et al. [7]. Both parent and mutant strains retained the ability to ferment lactose. The HH mutant IN-40 maps immediately upstream of an open-reading frame possessing no significant GenBank homologies.

Both the NH and HH transposon mutant expressed the carbohydrate group B antigen, produced equivalent amounts of the type

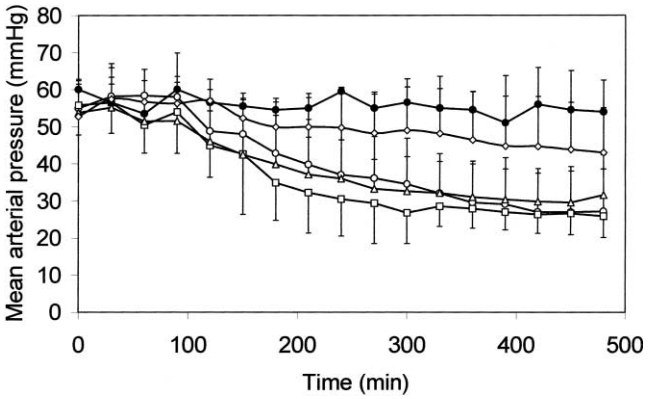

Figure 3. Mean arterial pressure of rabbits treated intravenously with 10^9 cfu of the COH1 (○), COH1-20 (△), COH1:*cyl* EΔ*cat* (◇), or IN40 (□) strain of group B streptococci. Control animals (●) received only PBS. Data are mean ± SD of all surviving rabbits per group ($n = 5–15$).

Table 1. Clinical chemistry monitoring of rabbit serum at different time points during experimental group B streptococcal (GBS) sepsis, by GBS strain.

Variable, time (min)	COH1	IN40	COH1-20	COH1:*cyl*EΔ*cat*
Red blood cell count, 10^6 cells/μL				
0	6.5 ± 0.6 (15)	6.7 ± 0.9 (15)	6.5 ± 0.6 (15)	6.2 ± 0.4 (12)
30	6.3 ± 0.5 (13)	6.5 ± 1.2 (12)	6.5 ± 0.9 (15)	6.1 ± 0.7 (12)
480	7.0 ± 0.8 (11)	6.3 ± 0.6 (5)	6.6 ± 1.0 (13)	6.3 ± 0.6 (12)
Hemoglobin level, g/dL				
0	12.8 ± 1.4 (15)	12.8 ± 1.6 (15)	12.4 ± 1.1 (15)	11.0 ± 0.7 (12)
30	12.4 ± 1.2 (13)	12.3 ± 1.7 (12)	12.4 ± 1.2 (15)	11.0 ± 0.9 (12)
480	13.4 ± 1.3 (11)	12.6 ± 1.8 (5)	12.6 ± 1.5 (13)	11.4 ± 1.0 (12)
White blood cell count, 10^3 cells/μL				
0	4.5 ± 1 (15)	4.5 ± 0.9 (15)	4.5 ± 1.1 (15)	4.2 ± 0.8 (12)
30	3.0 ± 1.8 (13)[a]	2.2 ± 0.9 (12)[a]	2.9 ± 1.3 (15)[a]	2.8 ± 0.5 (12)[a]
480	1.6 ± 0.7 (11)[a]	2.1 ± 1.2 (5)[a]	1.9 ± 0.9 (13)[a]	1.4 ± 0.9 (12)[a]
Platelet count, 10^3 cells/μL				
0	475 ± 155 (15)	400 ± 136 (15)	447 ± 175 (15)	396 ± 171 (12)
30	265 ± 101 (13)[a]	156 ± 93 (12)[a]	291 ± 133 (15)[a]	196 ± 99 (12)[a]
480	281 ± 108 (11)[a]	166 ± 121 (5)[a]	275 ± 132 (13)[a]	254 ± 96 (12)
Aspartate aminotransferase level, U/L				
0	16 ± 7 (15)	15 ± 6 (15)	11 ± 4 (15)	13 ± 5 (12)
480	164 ± 110 (11)[a]	3940 ± 2082 (5)[a]	127 ± 65 (13)[a]	71.3 ± 42.9 (12)[a]
Alanine aminotransferase level, U/L				
0	32 ± 9 (15)	27 ± 13 (15)	23 ± 8 (15)	26 ± 4 (12)
480	59 ± 14 (11)[a]	709 ± 517 (5)[a]	46 ± 19 (13)[a]	57.7 ± 39.1 (12)[a]
Creatinine level, mg/dL				
0	0.6 ± 0.4 (15)	0.5 ± 0.4 (15)	0.1 ± 0.05 (15)	1.1 ± 0.2 (12)
480	0.7 ± 1.1 (11)	2.4 ± 0.2 (5)[a]	0.5 ± 0.5 (13)[a]	1.1 ± 0.2 (12)
Lactate dehydrogenase level, U/L				
0	152 ± 123 (15)	107 ± 81 (15)	142 ± 112 (15)	ND
480	1043 ± 408 (11)[a]	7053 ± 3501 (5)[a]	1191 ± 413 (13)[a]	ND
Lactate level, mg/mL				
0	0.36 ± 0.15 (15)	0.42 ± 0.17 (15)	0.33 ± 0.11 (15)	ND
90	0.34 ± 0.21 (13)	0.43 ± 0.20 (12)	0.34 ± 0.09 (15)	ND
180	0.82 ± 0.29 (13)	1.3 ± 1 (11)[a]	0.5 ± 0.2 (15)[a]	ND
480	2.24 ± 1.5 (11)[a]	1.75 ± 0.91 (5)[a]	1.35 ± 0.79 (13[a])	ND
Nitrite concentration, μmol/L				
0	11.2 ± 5.2 (15)	11.4 ± 5.1 (15)	10.8 ± 5.7 (15)	ND
90	14.1 ± 3.6 (13)	15.8 ± 12.1 (12)	12.7 ± 3.8 (15)	ND
180	18.5 ± 6.3 (13)[a]	20.5 ± 8.2 (11)[a]	19.5 ± 10.5 (15)[a]	ND
480	32.2 ± 11.7 (11)[a]	47.5 ± 30.3 (5)[a]	32.5 ± 22.2 (13)	ND

NOTE. Data are mean ± SD of measurements for all surviving rabbits in each group (no. of rabbits). ND, not determined.
[a] $P < .05$, vs. the control measurements before injection of GBS (analysis of variance).

III–specific capsular polysaccharide, had equivalent hyaluronidase activity, exhibited comparable logarithmic growth in Todd-Hewitt broth and RPMI 1640 medium, and possessed identical enzymatic profiles and sugar fermentation patterns on the BioMérieux API 20 Strep identification system, compared with wt strain COH1 [11].

Very recently, the precise genetic basis of the GBS β-hemolysin, including the structural gene *cyl*E, has been defined as a result of heterologous expression of a GBS chromosomal library in *Escherichia coli* [10]. Targeted allelic exchange mutagenesis and complementation studies identified the gene *cyl*E as necessary for GBS β-hemolysin expression and sufficient to confer β-hemolysis to *E. coli*. Thus, *cyl*E appears to represent the structural gene for the GBS β-hemolysin. The precisely characterized NH mutant COH1:*cyl*EΔ*cat* [10] became available during the course of this project and showed attenuation of pathogenicity in the lapin model of septic shock similar to that of COH1-20, particularly with respect to mortality and liver toxicity. No isogenic HH GBS mutants have been produced as yet from manipulation of the *cyl* locus, so IN40 remains the best bacterial strain for examining the effects of overexpression of the β-hemolysin phenotype.

The results in the lapin model of septic shock indicate that expression of GBS β-hemolysin correlates well with high mortality and septic liver failure, whereas it does not aggravate hypotension or trigger massive NO release in this model. Mortality was 67% among animals given the HH strain IN40, although the bacterial load in surviving animals was lower than that in the wt

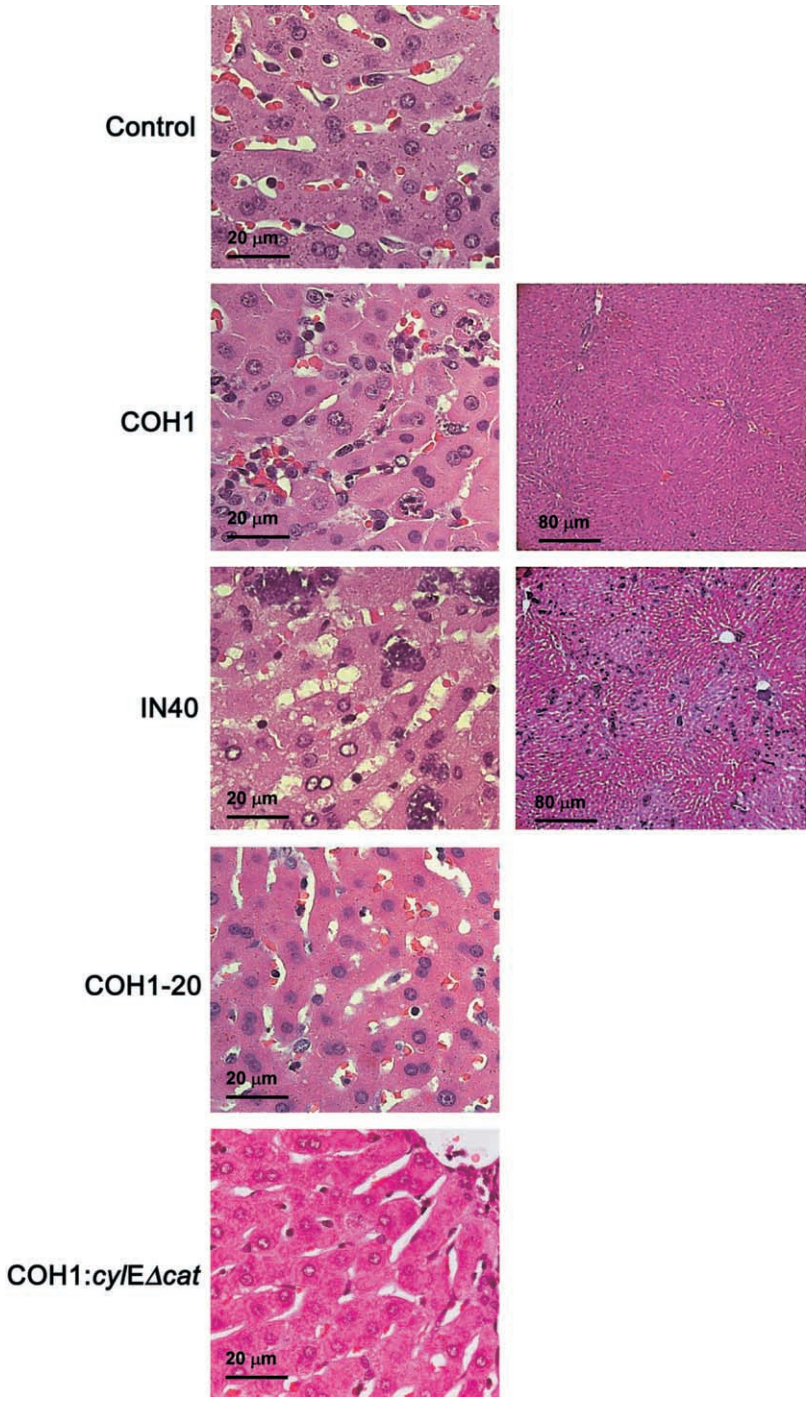

Figure 4. Histopathology of the liver demonstrated by hematoxylin-eosin staining 8 h after injection with either the COH1, IN40, COH1-20, or COH1:*cyl*EΔ*cat* strain of group B streptococci. Control animals were treated with PBS only.

treatment group, in which mortality amounted to 26%. It is possible that rabbits with higher levels of bacteremia with the HH strain died early, selecting a subpopulation of surviving animals with lower bacterial loads.

Since GBS β-hemolysin is a potent inducer of iNOS expression and NO production in murine macrophages in vitro [15], we initially hypothesized that the role of β-hemolysin in the pathogenesis of GBS sepsis might be to mediate massive release of NO from iNOS, resulting in severe hypotension. Surprisingly, both hypotension and the accumulation of nitrite (indicating NO production) in rabbits occurred to a similar degree in the wt strain COH1, HH mutant IN40, and NH mutant COH1-20

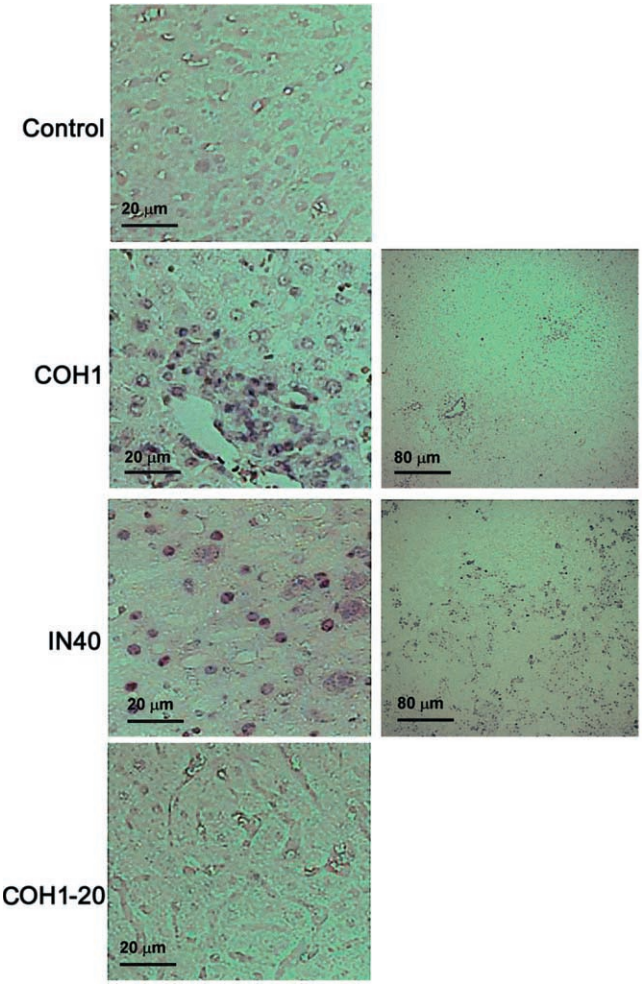

Figure 5. TUNEL staining of livers 8 h after injection with the COH1, IN40, or COH1-20 strain of group B streptococci. Control animals were treated with PBS only.

treatments groups, indicating that NO and hypotension do not explain the different mortality rates found in this model. One possible explanation for this discrepancy is that rabbit macrophages, in contrast to murine or bovine macrophages, fail to generate detectable amounts of NO byproducts after treatment with proinflammatory stimuli [24]. The β-hemolysin–independent increase of serum nitrite in rabbit serum might be due to NO release from other cell types (e.g., endothelial cells, Kupffer cells [KCs], or hepatocytes) [25]. Wang et al. [26] recently showed that the main source of iNOS-derived NO in a murine model of endotoxemic sepsis was parenchymal and not inflammatory cells. Using a murine model of systemic group A streptococcal infection, Sriskandan et al. [27] describe that iNOS was found in KCs and hepatocytes but not macrophages. Some of the NO released during GBS sepsis might be derived from the endothelial constitutive NOS or the brain NOS rather than iNOS. Hauck et al. [28] reported that intracerebroventricular GBS infection of newborn piglets up-regulated brain NOS and endothelial constitutive NOS in cerebral microvessels, whereas it did not trigger the expression of iNOS.

What, then, are the mechanisms by which GBS β-hemolysin exerts its detrimental effects on the outcome in this model of GBS septic shock? Organ dysfunction and injury play a pivotal role in sepsis mortality. There is precedent for pore-forming bacterial hemolysin-cytolysins in producing organ injury. *E. coli* β-hemolysin and *S. aureus* α-toxin are prototypes of a large family of pore-forming proteinaceous toxins that have been implicated in the pathogenetic sequelae of severe infection and sepsis, including development of thromboxane-mediated pulmonary vasoconstriction and edema formation, resulting in septic lung failure [29, 30].

To assess which organs might be targeted by GBS β-hemolysin, we performed clinical laboratory measurements, as used in clinical practice to monitor patients with sepsis. The marked in-

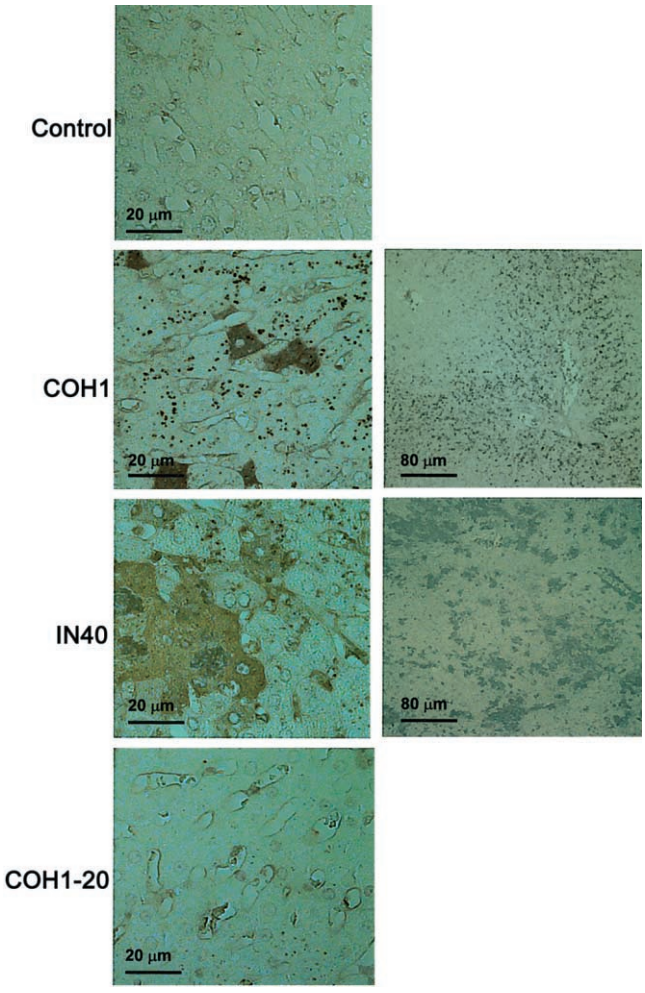

Figure 6. Activated caspase-3 staining of livers 8 h after injection with the COH1, IN40, or COH1-20 strain of group B streptococci. Control animals were treated with PBS only.

crease of transaminase activities in the serum of HH mutant IN40–treated rabbits is in accordance with the observation (made by use of a microscope) that mutant IN40 becomes sequestered in the liver parenchyma. Disseminated septic microabscesses associated with extensive necrotic areas were detectable in the liver after HH mutant IN40 treatment. The liver is an organ in which very high concentrations of bacteria are noted within KCs in primate and piglet models of GBS early-onset sepsis [31, 32]. In a gram-negative sepsis model, 50% of radiolabeled endotoxin injected intravenously was found in the liver within 5 min [33]. Our findings support the concept of the liver as a key component of host defense in systemic bacterial infections.

KCs represent the largest macrophage pool in the body and are chiefly responsible for microbial clearing from the blood [33]. Activated KCs produce proinflammatory mediators and reactive oxygen species and thus can initiate liver injury during endotoxemia. Hamada et al. [34] describe that, in endotoxin-treated rats, tumor necrosis factor (TNF)–α released by KCs causes hepatocyte apoptosis by activating caspases downstream of TNF receptor 1. In contrast, Wang et al. [35] describe that KCs and polymorphonuclear neutrophil granulocytes activated by gram-negative endotoxin or TNF-α induced significant hepatocellular necrosis, rather than apoptosis.

To assess whether apoptotic pathways are involved in GBS β-hemolysin–mediated hepatocyte injury, we performed TUNEL and immunohistochemical staining of activated caspase-3, using a monoclonal antibody. Caspases are cysteine proteinases specifically involved in the initiation and execution phases of apoptosis, and caspase-3 is a key effector caspase executing apoptosis induced by the death receptors Fas and TNF receptor 1 [36]. Hepatocytes positive by TUNEL and active caspase-3 were most abundant in the HH mutant IN40–infected group, less frequent in the wt strain COH1–infected group, and absent in the NH mutant COH1-20–infected group or the sham-treated rabbits (figures 5 and 6).

In the group infected with HH mutant IN40, apoptotic hepatocytes were distributed randomly throughout the liver acini, whereas the numerous microabscesses associated with hepatocyte necrosis were clustered in sections close to the portal triad (figure 4). This pattern of localization suggests that hepatocyte necrosis is caused by high concentrations of β-hemolysin, whereas apoptosis might be a more sensitive indicator of β-hemolysin–mediated hepatocyte injury, which is triggered by low-to-moderate doses of β-hemolysin. This interpretation is supported by the observation that caspase-3 activation and positive TUNEL staining were evident even in the group infected with wt strain COH1, in which hepatocyte necrosis was not found by H-E staining.

The results of this study indicate that β-hemolysin plays a key role for the outcome of GBS sepsis by contributing to high mortality, the establishment of bacteremia, and bacterial invasion of the liver and apoptotic, as well as necrotic, injury to hepatocytes. This study illustrates aspects of the complexity of septic shock and the shortcomings in our current understanding of the fundamental mechanisms of mortality in septic shock. Identifying effective adjuvant therapies for septic shock will require further research into these molecular mechanisms, particularly for gram-positive septic shock, which remains less well understood than endotoxin-mediated shock. Agents targeted to neutralize β-hemolysin toxicity would be of theoretical benefit to infants with GBS septicemia.

Acknowledgments

We thank John Killmar and William Mackert, for their technical assistance with the septic shock model, and Jerry Rehg, for review of the histopathology.

References

1. Bone RC. Gram-positive organisms and sepsis. Arch Intern Med **1994**; 154:26–34.
2. Rubens CE, Wessels MR, Heggen LM, Kasper DL. Transposon mutagenesis of type III group B streptococcus: correlation of capsule expression with virulence. Proc Natl Acad Sci USA **1987**; 84:7208–12.
3. Vallejo JG, Baker CJ, Edwards, MS. Roles of the bacterial cell wall and capsule in induction of tumor necrosis factor α by type III group B streptococci. Infect Immun **1996**; 64:5042–6.
4. Orman KL, Shenep JL, English BK. Pneumococci stimulate the production of the inducible nitric oxide synthase and nitric oxide by murine macrophages. J Infect Dis **1998**; 178:1649–57.
5. Bannan J, Visvanathan K, Zabriskie JB. Structure and function of streptococcal and staphylococcal superantigens in septic shock. Infect Dis Clin North Am **1999**; 13:387–96.
6. Crass BA, Bergdoll MS. Toxin involvement in toxic shock syndrome. J Infect Dis **1986**; 153:918–26.
7. Weiser JN, Rubens CE. Transposon mutagenesis of group B streptococcus β-hemolysin biosynthesis. Infect Immun **1987**; 55:2314–6.
8. Spellerberg B, Pohl B, Haase G, Martin S, Weber-Heynemann J, Lütticken R. Identification of genetic determinants for the hemolytic activity of *Streptococcus agalactiae* by ISS1 transposition. J Bacteriol **1999**; 181: 3212–9.
9. Spellerberg B, Martin S, Franken C, Berner R, Lütticken R. Identification of a novel insertion sequence element in *Streptococcus agalactiae*. Gene **2000**; 241:51–6.
10. Pritzlaff CA, Chang JCW, Kuo SP, Tamura GS, Rubens CE, Nizet V. Genetic basis for the β-haemolytic/cytolytic activity of group B streptococcus. Mol Microbiol **2001**; 39:236–47.
11. Nizet V, Gibson RL, Chi EY, Framson PE, Hulse M, Rubens CE. Group B streptococcal hemolysin expression is associated with injury of lung epithelial cells. Infect Immun **1996**; 64:3818–26.
12. Gibson RL, Nizet V, Rubens CE. Group B streptococcal β-hemolysin promotes injury of lung microvascular endothelial cells. Pediatr Res **1999**; 45:626–34.
13. Nizet V, Kim KS, Stins M, Jonas M, Chi EY, Nguyen D, Rubens CE. Invasion of brain microvascular endothelial cells by group B streptococci. Infect Immun **1997**; 65:5074–81.
14. Nizet V, Rubens CE. Pathogenic mechanisms and virulence factors of group B streptococci. In: Fischetti VA, Novick RP, Ferretti JJ, Portnoy DA, Rood JI, eds. The gram-positive pathogens. Washington, DC: American Society for Microbiology, **2000**:125–36.
15. Ring A, Braun JS, Nizet V, Stremmel W, Shenep JL. *Streptococcus agalactiae* β-hemolysin induces nitric oxide production in murine macrophages. J Infect Dis **2000**; 182:150–7.

16. Doran KS, Chang JCW, Benoit VM, Eckmann L, Nizet V. Group B streptococcal β-hemolysin/cytolysin promotes invasion of human lung epithelial cells and the release of interleukin-8. J Infect Dis **2002**;185: 196–203.
17. Puliti M, Nizet V, von Hunolstein C, Bistoni F, Orefici G, Tissi L. Severity of group B streptococcal arthritis is correlated with β-hemolysin expression. J Infect Dis **2000**;182:824–32.
18. Griffiths BB, Rhee H. Effects of haemolysins of groups A and B streptococci on cardiovascular system. Microbios **1992**;69:17–27.
19. Nizet V, Gibson RL, Rubens CE. The role of group B streptococci β-hemolysin expression in newborn lung injury. Adv Exp Med Biol **1997**; 418:627–30.
20. Wessels MR, Benedi V, Kasper DL, Heggen LM, Rubens CE. Type III capsule and virulence of group B streptococci. In: Dunny GM, Cleary PP, McKay LL, eds. Genetics and molecular biology of streptococci, lactococci, and enterococci. Washington, DC: American Society for Microbiology, **1991**:219–23.
21. Lacks S, Hotchkiss RD. A study of the genetic material determining an enzyme activity in pneumococcus. Biochem Biophys Acta **1960**;39: 508–17.
22. Hevel J, Marletta M. Nitric-oxide synthase assays. Methods Enzymol **1994**;233:250–8.
23. Braun JS, Novak R, Gao G, Murray PJ, Shenep JL. Pneumolysin, a protein toxin of *Streptococcus pneumoniae,* induces nitric oxide production from macrophages. Infect Immun **1999**;67:3750–6.
24. Jungi TW, Adler H, Adler B, Thony M, Krampe M, Peterhans E. Inducible nitric oxide synthase of macrophages: present knowledge and evidence for species-specific regulation. Vet Immunol Immunopathol **1996**;54: 323–30.
25. Spitzer JA. Cytokine stimulation of nitric oxide formation and differential regulation in hepatocytes and nonparenchymal cells of endotoxemic rats. Hepatology **1994**;19:217–28.
26. Wang LF, Mehta S, Weicker S, et al. Relative contribution of hemopoietic and pulmonary parenchymal cells to lung inducible nitric oxide synthase (iNOS) activity in murine endotoxemia. Biochem Biophys Res Commun **2001**;283:694–9.
27. Sriskandan S, Moyes D, Buttery LK, et al. The role of nitric oxide in experimental murine sepsis due to pyrogenic exotoxin A–producing *Streptococcus pyogenes.* Infect Immun **1997**;65:1767–72.
28. Hauck W, Samlalsingh-Parker J, Glibetic M, et al. Deregulation of cyclooxygenase and nitric oxide synthase gene expression in the inflammatory cascade triggered by experimental group B streptococcal meningitis in the newborn brain and cerebral microvessels. Semin Perinatol **1999**; 23:250–60.
29. Ermert L, Rousseau S, Schütte H, et al. Induction of severe vascular leakage by low doses of *Escherichia coli* hemolysin in perfused rabbit lungs. Lab Invest **1992**;66:362–9.
30. Seeger W, Bauer M, Bhakdi S. Staphylococcal α-toxin elicits hypertension in isolated rabbit lungs. J Clin Invest **1984**;74:849–58.
31. Bowdy BD, Aziz SM, Marple SL, et al. Organ-specific disposition of group B streptococci in piglets: evidence for a direct interaction with target cells in the pulmonary circulation. Pediatr Res **1990**;27:344–8.
32. Rubens CE, Raff HV, Jackson JC, Chi EY, Bielitzki JT, Hillier SL. Pathophysiology and histopathology of Group B streptococcal sepsis in *Macaca nemestrina* primates induced after intra-amniotic inoculation: evidence for bacterial cellular invasion. J Infect Dis **1991**;164:320–30.
33. Mathison JC, Ulevitch RJ. The clearance, tissue distribution, and cellular localization of intravenously injected lipopolysaccharide in rabbits. J Immunol **1979**;123:2133–43.
34. Hamada E, Nishida T, Uchiyama Y, et al. Activation of Kupffer cells and caspase-3 involved in rat hepatocyte apoptosis induced by endotoxin. J Hepatol **1999**;30:807–18.
35. Wang JH, Redmond HP, Watson RW, Bouchier-Hayes D. Role of lipopolysaccharide and tumor necrosis factor–α in induction of hepatocyte necrosis. Am J Physiol **1995**;269:G297–304.
36. Enari M, Talanian RV, Wong WW, Nagata S. Sequential activation of ICE-like and CPP32-like proteases during Fas-mediated apoptosis. Nature **1996**;380:723–6.